



**POLYTECHNIC UNIVERSITY OF BUCHAREST**

**Faculty of Transport**  
**Road Vehicles Department**

***Studies regarding the aerodynamic improvement  
of road vehicles***

*-Aerodynamic optimization of vehicles-*

***- PhD thesis summary -***

Scientific adviser: Prof.univ.em.dr.ing. Gheorghe Frățilă

Author: Eng. Laurențiu Ilea

Bucharest  
2023

## **Acknowledgements**

I am deeply grateful to the teachers who guided every step of the academic parcours, with professionalism, with understanding for the years of my youth. I especially appreciate the guidance offered by this thesis supervisor – prof. dr. ing. Gheorghe Fratila, a true example of dedication and professionalism, together with conf.dr.ing. Daniel Iozsa and prof. dr. ing. Mihaela Popa, without whom this work would not have been possible. I express my acknowledge and respect to the entire group of teachers and teaching staff from the Department of Road Vehicles of the Faculty of Transport, Politehnica University of Bucharest.

I appreciate the support and guidance offered by my fellow colleagues from Renault Technologie Roumanie, where I had the chance to apply and develop my automotive engineering knowledge and skills. Special thanks to my colleague dr. ing. Raluca Iovănel, for her direct guidance during the internship in the CFD numerical simulation team, associated with the SMART research program, a program that gave me the chance to complete this study.

Last but not least, I thank my parents, wife and son for being by my side and helping me overcome difficult moments.

## **Keywords**

Aerodynamics of intervention vehicles

Aerodynamic optimization

Reduction of polluting emissions for road vehicles

CFD study for vehicle aerodynamics

# **TABLE OF CONTENTS OF THE PAPER**

## **1. INTRODUCTION**

- 1.1. AERODYNAMICS IN THE AUTOMOTIVE INDUSTRY
- 1.2 OBJECTIVES OF THE THESIS
- 1.3 THESIS STRUCTURE

## **2. AERODYNAMICS OF ROAD VEHICLES**

- 2.1 AERODYNAMIC PRINCIPLES OF ROAD VEHICLES
  - 2.1.1 STREAMLINES
  - 2.1.2 AIR PRESSURE
  - 2.1.3 AIR DENSITY
  - 2.1.4 AIR VISCOSITY
  - 2.1.5 REYNOLDS NUMBER
  - 2.1.6 BOUNDARY LAYER
  - 2.1.7 DRAG COEFFICIENT
  - 2.1.8 BERNOULLI'S EQUATION
  - 2.1.9 GENERAL PRESSURE DISTRIBUTION NEAR A VEHICLE
- 2.2 EVALUATION OF AERODYNAMIC FORCES
- 2.3 METHODS FOR MEASURING AERODYNAMIC RESISTANCE OF VEHICLES
- 2.4 WIND TUNNEL METHOD
  - 2.4.1 TYPES OF WIND TUNNELS
  - 2.4.2 CHALLENGES IN WIND TUNNEL DESIGN
  - 2.4.3 ADVANTAGES AND DISADVANTAGES OF MEASUREMENTS IN WIND TUNNELS
- 2.5 REFERENCE VEHICLES IN AERODYNAMIC HISTORY

## **3. CURRENT STATE OF THE STUDIED ISSUE**

- 3.1 VEHICLE CHARACTERISTICS AFFECTING AERODYNAMIC FORCES
  - 3.1.1 VEHICLE DIMENSIONS
  - 3.1.2 VEHICLE DESIGN
  - 3.1.3 GENERIC AERODYNAMIC ACCESSORIES
- 3.2 LITERATURE REVIEW

## **4. MATHEMATICAL MODELS FOR CFD SIMULATIONS**

- 4.1 NAVIER-STOKES EQUATIONS
- 4.2 TURBULENCE AND MODELING APPROACHES
- 4.3 REYNOLDS-AVERAGED NAVIER-STOKES (RANS) METHOD
- 4.4 DIRECT NUMERICAL SIMULATION (DNS) METHOD
- 4.5 K-E TURBULENCE MODEL

- 4.6 REALIZABLE K-E TURBULENCE MODEL
- 4.7 K- $\Omega$  TURBULENCE MODEL
- 4.8 DETACHED EDDY SIMULATION (DES) MODEL
- 4.9 LARGE EDDY SIMULATION (LES) MODEL
- 4.10 LATTICE BOLTZMANN METHOD

## **5. DETERMINATION OF AERODYNAMIC FORCE THROUGH CFD METHOD**

- 5.1 COMPUTER-AIDED DESIGN (CAD) MODEL
- 5.2 TESTING ENVIRONMENT
- 5.3 DISCRETIZATION OF THE VIRTUAL TESTING ENVIRONMENT
- 5.4 BOUNDARY CONDITIONS
- 5.5 CONVERGENCE OF CFD SIMULATION RESULTS
- 5.6 AERODYNAMIC RESULTS FOR STUDIED MODELS, WITHOUT LIGHT WARNING DEVICE
- 5.7 AERODYNAMIC RESULTS FOR STUDIED MODELS, WITH LIGHT WARNING DEVICE
- 5.8 STUDIES FOR IMPROVING THE AERODYNAMIC PERFORMANCE OF INTERVENTION VEHICLES
- 5.9 INFLUENCE OF LATERAL WIND ON VEHICLE AERODYNAMICS
- 5.10 CFD RESULTS FOR OPTIMIZED AERODYNAMIC INTERVENTION VEHICLES
- 5.11 STUDIES ON LIGHT WARNING DEVICES FOR TRUCKS

## **6. EXPERIMENTAL RESULTS**

## **7. CONCLUSIONS, PERSONAL CONTRIBUTIONS, AND FUTURE RESEARCH DIRECTIONS**

- 7.1 FINAL CONCLUSIONS
- 7.2 PERSONAL CONTRIBUTIONS
- 7.3 FUTURE RESEARCH

NOTATIONS USED

LIST OF ABBREVIATIONS

BIBLIOGRAPHY

## **1. INTRODUCTION**

To ensure an efficient and clean transport system (commercial or non-commercial), legislative bodies introduced the first set of rules [1] on car emissions several decades ago, with the aim of reducing the effects of pollution on humans and the environment [2]. The automotive industry has thus begun a transformation process that is still ongoing. Due to the great diversity of factors and complexity of the issue, the topic is intensely disputed in the industry but also in the academic world. Even though important developments are seen in areas such as powertrain technology, vehicle design, materials technology, etc., solutions still exist to improve vehicle performance, and engineers are working daily to find them and make them available to vehicle users.

In this context, the current paper seeks, by means of CFD, to improve the aerodynamic performance of intervention vehicles. These special vehicles are most frequently exempted from emission standards for road vehicles [4], but contribute to urban and suburban air pollution, in particular due to the warning devices mounted on their roof. The practical study was organized into 3 parts. The first part focuses on assessing the aerodynamic performance of three body types, respectively those that are most frequently used by authorities and intervention forces – sedan, hatch back and SUV. The second part will determine the aerodynamic influence of the light warning devices in different use cases and, finally, the third part aims to improve the performance of special vehicles by adding additional parts to compensate for the degradation generated by the presence of the light warning device.

In anticipation of a possible evolution of legislation on setting a maximum emission level for special vehicles, the objective of the thesis is to assess the aerodynamic resistance of vehicles equipped with roof warning devices and to identify possible and easy to implement technical solutions to reduce their negative impact on aerodynamic performance. Thus, it is intended to identify accessories that could be easily mounted on special intervention vehicles to cancel the effect of the light warning device on aerodynamic performance and to obtain the same aerodynamic performance as the base vehicle, the one without the light warning device.

## **2. AERODYNAMICS OF ROAD VEHICLES**

The chapter details the basic laws governing the interaction between a moving object and a fluid, in this case a vehicle moving through air.

Experiments and studies conducted for automotive dynamics have shown that, in addition to the forces in the contact zone, there is always an exchange of forces that occurs between the vehicle body and the air surrounding it. As powertrains evolved, and as a direct consequence the average speed increased, both drivers and scientists noticed that the car became less efficient at high speeds, and fuel consumption was significantly higher.

The force imprinted by the air in which the object moves on it is defined as aerodynamic drag and it has two main components, a frictional force and a pressure force. The main notions described in this chapter are: Current lines, Air pressure, Air density, Air viscosity, Reynolds number, Boundary layer, Friction coefficient, Bernoulli relation.

Based on the fundamental concepts of aerodynamics, the overall pressure distribution in the body area of a vehicle can be analysed. Turbulent resistance is given by the turbulent air -flow from the rear area of the vehicle and is influenced by its shape as well as by the pressure difference between the front and rear of the vehicle. The way in which the phenomenon of air separation occurs leads both to the amplitude of turbulent resistance and to the increase of the associated shape. Turbulent flow is time-dependent, in a periodic manner (if external factors are constant). This generates a pulsating phenomenon that can have very high amplitudes and affects the stability of other vehicles, for example in trucks.

The pressure (perpendicular to the surface of the vehicle body) and the friction force (parallel to the air flow) give rise to the overall aerodynamic resistance and can, for the purpose of the study, be expressed through a spatial system consisting of 3 axes (OX, OY, OZ), based on which the drag coefficient can be expressed.

$$C_D = \frac{D}{\frac{1}{2}\rho V_\infty^2 A} \quad C_L = \frac{L}{\frac{1}{2}\rho V_\infty^2 A} \quad C_Y = \frac{Y}{\frac{1}{2}\rho V_\infty^2 A}$$

To determine the aerodynamic drag of a motor vehicle, it is necessary to determine the force that must be developed by the power unit to leave the state of rest. The paper details some of the main methods applied over time to research this force and associated difficulties, namely: measurements made on the track, with the vehicle isolated from the environment, application of a network of pieces of wire with a free end, deceleration time method on the track, measurements made in different types of wind tunnel.

The idea associated with the wind tunnel is to approach the whole phenomenon studied from another perspective, namely, the vehicle does not move through the air, but the air moves around the vehicle. Starting from this premise, the idea of an enclosure was developed, in the centre of which is the studied object, the vehicle, while the air is moved by high-power fans.

The main advantages associated with this method are:

- (i) all devices necessary for measurements need no longer be carried on board because the vehicle is stationary,
- (ii) the speed of the draught can be controlled perfectly in relation to the vehicle,
- (iii) pressure and temperature can be precisely controlled,
- (iv) experiments are carried out under the same conditions and can be easily duplicated,
- (v) the time required to prepare for a new session is relatively short.

Some of the most representative examples of vehicles with an aerodynamic design are presented in this subchapter to highlight the evolution that has taken place over the last century, in terms of aerodynamics, as well as current performance.



**Figure 1** model La Jamais Contente, Stanley Steamer Rocket, Rumpler Tropfenwagen, Aurel Persu's aerodynamic vehicle

Figure 1 shows 'La Jamais Contente', the first electrically powered vehicle which exceeded 100km/h in 1899. After only 7 years, steam propulsion and an aerodynamic body allowed the 'Stanley Steamer Rocket' to reach and exceed the 200 km/h threshold. The great benefits of aerodynamic science were proven by Rumpler "Tropfenwagen", from 1921, having a design similar to the shape of a drop of falling water.

An outstanding example of the same principle, with a patented design in 1922, is the vehicle created by the Romanian engineer, Aurel Perșu, which could not accommodate the same number of passengers as the Rumpler but had a Cd value of only 0.22. Currently, one of the best performing vehicles for several passengers is the Light year, from 2022, with a drag coefficient of just 0.175.

### 3. THE CURRENT STATE OF THE STUDIED ISSUES

There are 3 main characteristics which, with the right approach, can have an important positive influence on controlling and reducing aerodynamic drag: vehicle dimensions, vehicle shape and specific accessories that influence the air-flow around it.

A key factor influencing aerodynamic drag is the size of the vehicle. The rear surface of the vehicle is directly related to the initial size of the rear wake, which means that if we are trying to reduce the size of the rear wake, the rear area should be minimal. The best results for the CdA parameter are obtained for vehicles that mimic by design the shapes of the droplet of falling water, i.e. with the smallest possible rear surface.

The second characteristic of the car that has an influence on aerodynamic force is, of course, its design. The overall aim is to minimise local resistance to the front of the vehicle, ensure rapid reattachment of air-flow and maintain stable air-flow near the body panels for as long as possible until air reaches the rear surface of the vehicle [37].

In the case of motor vehicles, the technical accessories used to reduce aerodynamic drag vary according to size, shape and mounting position. They are developed specifically for each vehicle. The aim is to control the airflow around the vehicle (i.e. on both sides and in the lower area and upper part of the vehicle) to control the shape and size of the rear wake.

Therefore, drawing general conclusions for the hatch back segment simply by extrapolating measurements to a specific hatch back model may lead to significantly different results and thus erroneous conclusions. In this context, considering all these constraints, the study focuses on a specific, generically chosen model, and conclusions are adopted accepting possible dispersions in the conclusions found for the respective class of vehicles.

The generally used fixed aerodynamic accessories are represented by deflectors (rear, and rear side, wheels) and fairings (engine, centre, rear axle). The rear deflector and rear side deflectors are designed to control the detachment point at a specific coordinate, which is precisely adjusted for a balanced rear wake. Aerodynamic fairings are specially designed to cover most of the area of the lower body area, with a flatness coefficient as close as possible to 100%. In addition to fairings designed to ensure uniformity of airflow under the vehicle, aerodynamic deflector elements can also be placed underneath the vehicle. To compensate for the wheel side wake, manufacturers have added open arches on the sides of the front bumper. These arches take over high-energy airflow from the front of the vehicle and reduce the size of the side wheel wake.



In addition to the traditional elements mentioned, there are also more widely available active aerodynamic elements such as: active front wheel deflectors, active rear diffuser, front grille fins, active rear deflector and active wheel covers.

All of the above elements, fixed or active, have a variety of shapes, sizes and give different results depending on their application. In addition to these, which are the main elements analysed from an aerodynamic point of view, each exterior element is examined to maximise the efficiency of movement. The shape and size of the exterior mirrors, if not already replaced by small cameras, aerodynamic wheels, even the aerodynamic design of the tires, as little space as possible between the body panels or additional masks on the front air inlets are just some of the other elements that are continuously optimized for better performance.

All this effort is a direct consequence of the current context in which, on one hand, legislation imposes a strict level of emissions and, on the other hand, customers are more attentive to fuel consumption but also to the influence of the vehicle used on the environment.

The literature confirms that the influence of light warning devices when fitted to ambulance-type vehicles [50] indicates a similarity between the results obtained in the CFD environment and in the wind tunnel on a small scale using the applied wire method. Yorkshire's Ambulance Service Trust (YAST) fleet has 1500 ERVs moving 40 million miles each year (~64.4 million kilometres), resulting in 4.2 million litres of fuel at a cost of over £6 million.

These studies briefly presented in the paper bring to attention a careful selection of relevant literature on the benefits of aerodynamic design and the possible improvement of fuel economy for commercial vehicles. Another valuable source of information was identified to be the work of Ali Reza Taherkhani [53] which starts from basic theoretical notions. The paper indicates the evolution of the Cd value for different vehicles, demonstrating the important benefits of aerodynamic optimization - the average drag coefficient of HGVs (vehicles transporting commercial goods) which was 0.7 in the 1920s, while today this value is reduced to about 0.5.

Regarding the heavy vehicles with trailers, the overall reduction in drag could reach 23% when combining extended side fairings, aerodynamic fairings, extension surfaces at the rear of the trailer and covering of areas between the wheels [55]. Aider indicates that a drag reduction of 25.2% is achieved through a combination of additional devices from those mentioned on different areas of the vehicle.

Although the conclusions found are consistent with those of the current paper, no specific study has been identified on the light warning devices for the currently analysed body types (sedan, hatch back, SUV), nor their influence on aerodynamic performance. Therefore, the

results obtained following this study and detailed in the paper are all the more important for the field of aerodynamics of intervention vehicles (vehicles with a light warning device on the roof).

#### 4. MATHEMATICAL MODELS FOR CFD SIMULATIONS

The CFD method or method of calculating fluid dynamics is the main working tool currently used by aerodynamic engineers. The mathematical method for predicting the flow of a fluid is successfully used in the study of vehicle aerodynamics. It should be remembered that the basis of fluid flow modelling is the Navier-Stokes set of differential equations. The solution can be obtained through a direct or probabilistic approach.

To model complex flows, it is necessary to introduce some simplifications into the system of equations. These come in the form of turbulence patterns such as k-epsilon, k-omega, etc.

Another method involves replacing the direct solution of the system of equations with the probabilistic approach proposed by Boltzmann. Thus, by parameterizing a family of probabilistic functions, fluid behaviour can be modelled from the perspective of the fluid component of a multitude of particles that can move in a given lattice, hence the name of the Lattice-Boltzmann method. Both methods are used by software programs that are used to evaluate the aerodynamic performance of cars.

Information systems have seen a multitude of applications, including in the field of engineering. To theoretically study the flow of fluids and air in the aerodynamics of motor vehicles, the Navier-Stokes equations are used. These are described as follows:

$$\begin{aligned} \frac{\partial(\rho u)}{\partial t} + \frac{\partial(\rho u^2)}{\partial x} + \frac{\partial(\rho uv)}{\partial y} + \frac{\partial(\rho uw)}{\partial z} &= -\frac{\partial p}{\partial x} + \frac{\partial}{\partial x}(\lambda \nabla \\ V - 2\mu \frac{\partial u}{\partial x} \left[ \mu \left( \frac{\partial v}{\partial x} + \frac{\partial u}{\partial y} \right) \right] + \frac{\partial}{\partial z} \left[ \mu \left( \frac{\partial u}{\partial z} + \frac{\partial w}{\partial x} \right) \right] + \rho f x \\ \frac{\partial(\rho v)}{\partial t} + \frac{\partial(\rho uv)}{\partial x} + \frac{\partial(\rho v^2)}{\partial y} + \frac{\partial(\rho vw)}{\partial z} &= -\frac{\partial p}{\partial y} + \frac{\partial}{\partial x} \left( \mu \frac{\partial u}{\partial x} \left[ \mu \left( \frac{\partial v}{\partial x} + \frac{\partial u}{\partial y} \right) \right] \right) + \frac{\partial}{\partial y} (\lambda \nabla V + \\ 2\mu \frac{\partial v}{\partial y}) + \frac{\partial}{\partial z} \left[ \mu \left( \frac{\partial w}{\partial y} + \frac{\partial v}{\partial z} \right) \right] + \rho f y \\ \frac{\partial(\rho w)}{\partial t} + \frac{\partial(\rho uw)}{\partial x} + \frac{\partial(\rho vw)}{\partial y} + \frac{\partial(\rho w^2)}{\partial z} &= \frac{\partial p}{\partial z} + \frac{\partial}{\partial x} \left( \mu \left( \frac{\partial u}{\partial z} + \frac{\partial w}{\partial x} \right) \right) + \frac{\partial}{\partial y} \left[ \mu \left( \frac{\partial w}{\partial y} + \frac{\partial v}{\partial z} \right) \right] + \\ \frac{\partial}{\partial z} (\lambda \nabla V + 2\mu \frac{\partial w}{\partial z}) + \rho f y \end{aligned}$$

The system consists of non-linear, coupled and partially differential equations. These properties make it impossible to find an analytical solution [8]. One method of approach in identifying Navier-Stokes solutions is the numerical model.

One of the essential steps in parameterizing a CFD simulation is to define the fluid turbulence model. This action has a direct impact on the nature of the results and error in relation to the actual phenomenon. Ideally, an attempt is made to solve a complex flow with a turbulence pattern as simple as possible for minimal resource consumption.

Turbulence is a time-varying phenomenon. Another important feature is that eddy stress structures move along the flow, having a relatively long service life. For this reason, certain turbulence cannot be characterized as local. Thus, the upstream flow is of vital importance for the flow in the analysed area.

To characterize the turbulence component, several models with different approaches have been created: either by approximating the solution of the RANS equations or by solving them directly.

For RANS models:

*a. Eddy viscosity model (eddy viscosity model – EVM)*

In this model, it is assumed that the effort associated with turbulence is proportional to the average stress rate. Wake viscosity is derived from the turbulent transport equation.

*b. Nonlinear eddy viscosity models (eddy viscosity nonlinear models – NLEVM)*

Turbulence effort, in this case, is modelled as a nonlinear function of mean velocity gradients. Turbulence scaling is determined by solving transport equations. This model is used to highlight turbulence associated with certain types of efforts.

*c. Differential stress models (DSM)*

This category consists of Reynolds stress transport models or second-order closure models (closure models - SOC).

When it comes to calculating fluctuating quantities, the following methods are available:

*a. Macroscopic eddy simulation (large eddy simulation - SLE)*

This involves calculating the variation of flow over time, modelled on subnet-level interactions.

*b. Direct simulation method (direct numerical simulation – DNS)*

This method is not based on modelling, but on the direct calculation of the entire flow. [57]

A different approach is the method based on the principles proposed by Ludwig Boltzmann [61]. His major contribution was the development of statistical mathematics that explains and predicts how the properties of atoms can determine the physical properties of matter (such as viscosity, thermal conductivity, and diffusion). He laid the foundation for kinetic theory and the Maxwell–Boltzmann distribution of the velocities of molecules of a gas.

From the automatic lattice gas method derives the Boltzmann network method currently used by CFD software. The main advantage compared to the previous method is noise compensation by the statistical approach. According to the theoretical principles described, by means of kinetic theory, the state of the fluid is described by a Newtonian method to identify the position and speed of molecules. The application of the Boltzmann method is also possible on non-Newtonian fluids, but the complexity of the mathematical model needs to be increased.

For the study of the flow of a fluid in three-dimensional space (such as the air-flow currents in a room), the model D3Q19 is used, which is successfully applied for Reynolds numbers in the subunit Mach spectrum and with isothermal properties. This is a hybrid, particle-based, continuous method. Complex modelling through the details of the particle-particle collision or its expansion level can be successfully applied to parallel computational architectures. In this way, a significant reduction in the need for resources and reduction of the time required to perform a simulation is achieved.

## **5. DETERMINATION OF AERODYNAMIC FORCE BY CFD METHOD**

The CFD method began to be widely used by all manufacturers in the development phase of a new project due to its multiple benefits, such as: the possibility of performing several iterations in a short period of time, a relatively faster setup of the experiment compared to the physical one, a significantly reduced budget for the CFD experiment compared to the physical one, possibility to view the airflow with the CFD instrument.

Given the objective of the work and definition of special vehicles, the CFD method chosen requires a base vehicle to which, at a successive stage, a warning light device will be added, thus following the real-life scenario.

In order to ensure minimal representativeness, but also to focus a reduced variety, the study was conducted on three generic body types that were considered to be the most commonly used as special vehicles: hatch back body type, sedan body type and SUV body

type. While this simplifying assumption reduces the resources required and the possible variety of results, aerodynamic drag is extremely sensitive not only to body type, but also to small variations in dimensions and, of course, body design. Thus, a second simplifying assumption was necessary, namely the choice of a specific design for each body type mentioned, taking into account the fact that the results obtained will not be able to be applied precisely for the whole category, but will allow to obtain an overview of the aerodynamic influence of the fitting of a light warning device, but not the exact values.

In the light of those two assumptions, the vehicles chosen are illustrated in Figure 2.



**Figure 2** CAD model of SUV

Given this test environment and its characteristics, the virtual experiment is built using the same proportions and functional devices specific to the wind tunnel. The test chamber is assembled from an insulated entrance and exit with side walls, a floor and a ceiling. The object under study is located at an equal distance from the side walls.

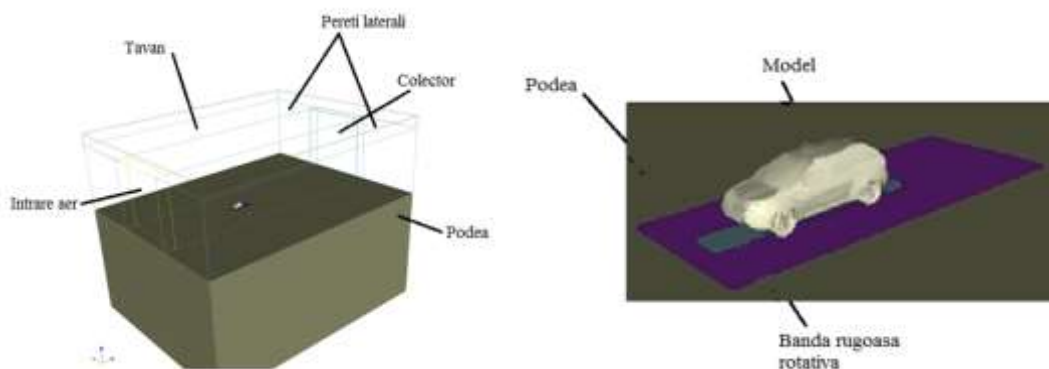


**Figure 3** Virtual test setup [60]

The CAD model is located near the air inlet area and further from the outlet to allow for more accurate measurement of the rear wake.

Volume meshing is achieved by using a hybrid method between the two methods, manual and automatic. Thus, the program is parameterized to have the finest dimension (cells with a

length of 2mm) next to the vehicle while near the walls a higher level (cells with a length of 64mm), the passage being made with a multiplication of 2 to facilitate the convergence process. The results are recorded in each cell and assembled to visualize pressure, speed, wake and numerical drag coefficient by applying the Lattice-Boltzmann mathematical model.

While the boundary conditions for fixed elements, such as walls, entrance and exit, are defined with fixed numerical values, all boundary conditions related to the studied object are defined according to its specific parameters, such as length, width, wheel coordinates, and, accordingly, the definition of resolution ranges is amplified in order to finally obtain a relevant result.

To reduce the simulation error, the user must identify a time step from which convergence oscillations are reduced. The CFD simulation performed in the current paper uses 250,000 iterations, since this value allows for a stabilized convergence curve on this type of model. Also, all simulations were averaged from 100,000 iterations, due to relatively large oscillations in the first area of the graph.

The first stage of the research was to determine the basic aerodynamic performance of the three body types studied (hatch back, sedan and SUV). Models imitate real cars as much as possible, considering the design, dimensions, and also technical parts located under the body.

**Table 1** Aerodynamic performance for base vehicles expressed in CDA

Case studied	Area (A)	CdA [m <sup>2</sup> ]
Body type : sedan	2.240m <sup>2</sup>	0.659
Body type :hatch back	2,390m <sup>2</sup>	0.836
Body Type : SUV	2,445m <sup>2</sup>	1.000

A comparison of the reference values of the CdA indicates, as expected, that a sedan body has the best aerodynamic performance, while the SUV body type has the highest CdA value. The main factors that lead to these results are the shape and size of the rear of the vehicle, as well as its riding height, elements that have a direct influence on the energy level of the rear wake.

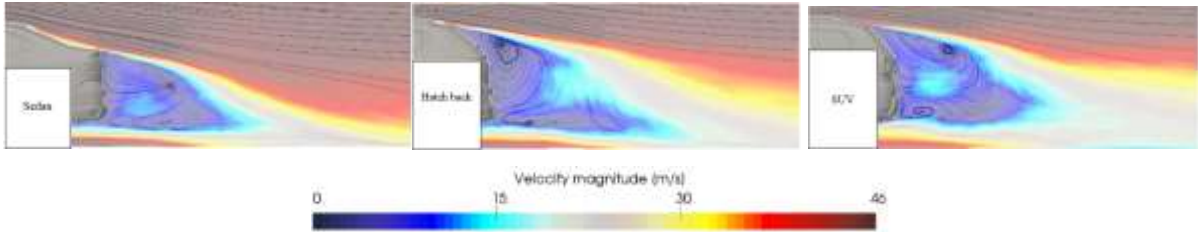


**Figure 4** Rear wake represented by current lines and magnitude of speed [70]

Since the sedan body type has a smaller surface area at the rear and its shape is more similar to a drop of falling water, the rear wake is smaller in height and even length, which indicates smaller overall dimensions. For cars with hatch back and SUV bodies, the characteristics of the body determine the creation of a much larger wake in the Z direction, which is more difficult to dissipate. Because of this, it has a larger size in the X direction. It can be seen that, although not significant, the rear wake of the SUV body is larger than the rear wake of the car with the hatch back body.

The second step in carrying out the study was to evaluate the aerodynamic performance of the same vehicles, but with the addition of the warning light device on their roof. For obtaining the best image on the possible performance dispersion, the warning device shall be mounted in the forward position (case "i"), middle position (case "ii") and rear position (case "iii"). For this purpose, an arbitrary device was chosen in shape and size, even though there is a great diversity in the design of the warning device, as well as variations in its geometry.



**Figure 5** Mounting positions for warning device

With the warning device added, the CdA value increases from +5.8% to +37%, depending on the vehicle type and mounting position. The greatest influence is recorded for the sedan body, with the warning device mounted in the forward position. The airflow is very turbulent, since the device is placed directly in the path of high-speed airflow coming from the windshield area. This technical definition will increase the value of carbon dioxide produced by approximately +12 g CO<sub>2</sub>/km. The best solution for the sedan body turns out to be the middle mounting position, with an additional +0.094 m<sup>2</sup> in the CdA value and an increase in the value of carbon dioxide produced by +5 g CO<sub>2</sub>/km. In this case, the warning device is not in the way of the windscreen's high-speed airflow, so that the associated wake is not added to the rear

wake of the same amplitude. The rear-mounting position will increase the value of carbon dioxide produced by +6.5 g CO<sub>2</sub>/km.

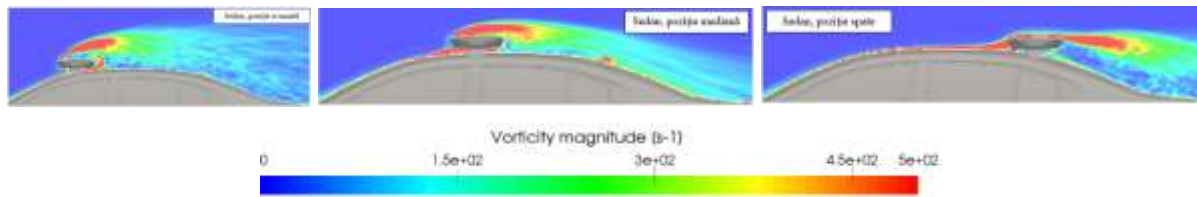


**Figure 6** Magnitude of vorticity for sedan body with warning device

Applying the same type of analysis to the hatch back body, it resulted that the warning device brings a degradation between +8.2% (case "iii") and +19% (case "i"). It should be noted that the middle and rear mounting positions can be treated as generating the same results. This conclusion arises due to the small difference in the value of CdA when the CFD error is also considered.

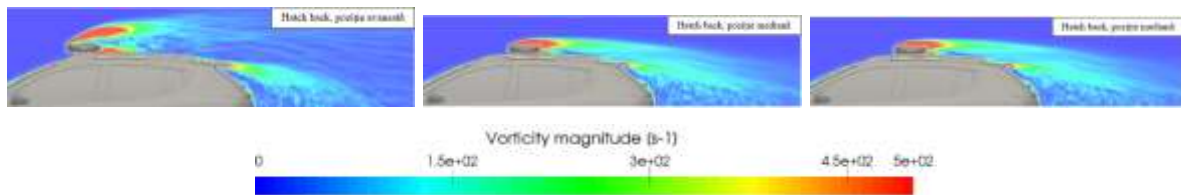


**Figure 7** Magnitude of vorticity for hatch rear body with warning device

It can be concluded that, due to worse natural wake of hatch back bodies (compared to sedans), the influence of the light warning device on the CdA value is lower, with a total difference in carbon dioxide emissions of 1.5 g CO<sub>2</sub>/km for the best-case scenario, respectively 4 g CO<sub>2</sub>/km for the worst-case scenario.

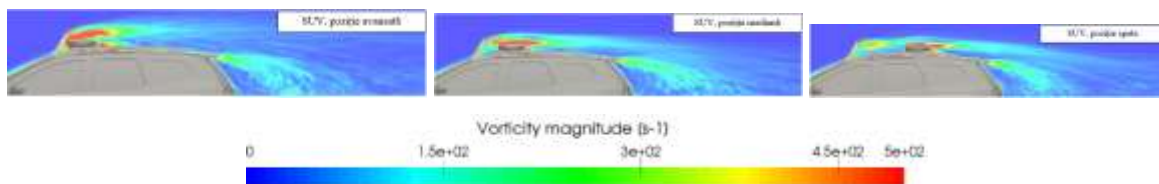


**Figure 8** Magnitude of vorticity

Given the results described above, step 3 presents the challenge of reducing the aerodynamic influence of the warning device by adapting or adding new aerodynamic accessories. The basic criterion is that the modification is minimal for maximum benefit so that



the study can be used for the practical application of the solutions identified. Elements considered to be easy to add to improve aerodynamics are wheel accessories (rim, wheel trim) and fairings under the body.

The wheels were studied specifically, on the same body types, to assess the benefit of CdA that could be obtained. Two factors chosen to be studied are the flatness and porosity of the wheel design.

To assess the impact of rim porosity on overall strength, an analysis was carried out using 7 different configurations - (P): 2.3%, 3.32%, 17.64% (existing solutions), 50%, 35%, 15% and 0% (proposed solutions)

The configuration of the steel rim and wheel cap gives a performance of 0.388 for the drag coefficient and is considered the reference. After removing the cap, the CdA value is improved by 0.004. The gain is even more significant (0.023) after replacing the steel rim and cap with an alloy wheel. The bottom line is that from an aerodynamic point of view, the alloy wheel configuration under consideration (case 3) is the most efficient. The superior properties of the material used allow engineers to have better shape control and therefore better control over the airflow.

The next step after evaluating existing generic solutions is to check what happens if wheel openings are gradually reduced in size. For this purpose, one fully closed cap ( $P = 0\%$ ), one relatively maximum open cap ( $P = 50\%$ ) and two intermediate solutions ( $P = 35\%$ ,  $P = 15\%$ ) were tested under the same conditions as the first 3 cases.

The best result is achieved when using the full cap ( $P = 0\%$ ), while the worst result is obtained for the most open cap.

Compared to the steel rim, with or without a wheel cap, the alloy rim has better aerodynamic results. As regards the possibility of integrating a more enclosed wheel cap or even an active wheel cap, the present study identified the best result for a zero porosity solution. With an overall gain of 0.033 relative to the standard steel rim and 0.005 relative to alloy wheels, the fully enclosed wheel cap is considered to be a good approach for a reduction in overall CdA.

As highlighted, the zero-porosity wheel cap can also bring benefits from an aero-acoustic point of view. The main negative impact that has not been studied in this work, but which could prevent the implementation of this solution is the brake cooling. The evolution towards hybrid and electric vehicles also involves a remodelling of the braking system, so this impediment could also be overcome.

The rear wheel covering should theoretically limit the rotational airflow around the wheel, reduce the local lateral wake in the Y direction, and allow longitudinal airflow to follow a smooth path from the front door to the rear wing of the vehicle. Thus, in a first phase, the size of the mask was assessed. The best Cd result is obtained for the fully enclosed wheel arch with a delta of 0.024 compared to a standard configuration. Cases 2 and 3 show the trend of decreasing drag coefficient with increasing wheel arch mask.

**Table 2** CFD results of wheel arches for the base vehicle

Setup no.	Cazul 1	Cazul 2	Cazul 3	Cazul 4
Cd	0.377	0.367	0.364	0.353
$\Delta Cd$		0.011	0.013	0.024
Reprezentare vizuala				
Descriere	Caz standard	Pasaj inchis pana la nivelul pneului	Pasaj inchis pana la nivelul capacului	Pasaj complet inchis

In the second phase, three different configurations of the full mask were compared – right rear edge, curved back edge and straight rear edge plus cutting area. CFD simulations indicate that case 4 is aerodynamically more favourable than case 5 due to a lower pressure value behind the wheels.

While the impact of the baffles was reduced compared to the full mask, the detailed study showed that the profiled deflector having the same height as the right one brought the greatest gain [74].

The sensitivity of vehicle aerodynamics to crosswind is studied for a hatch back vehicle at an angle ( $\alpha$ ) between  $-20^\circ$  and  $+20^\circ$  deviation from vehicle axis X, as graphically described in Figure 9. These values were chosen due to the high frequency of occurrence in real life, as shown by some studies.

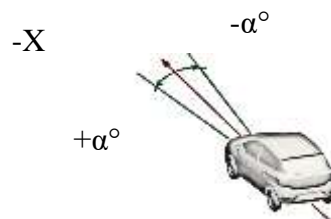


**Figure 9** Definition of vehicle coordinate system, for the study of crosswind

A first set of results, plotted in figure 10, shows that for  $0^\circ < \alpha < 2^\circ$ , the drag coefficient is relatively constant. This is followed by a gain of 0.025 units for  $4^\circ < \alpha < 6^\circ$ . At about  $8^\circ$ , an inflection in the Cd variation is observed. For  $10^\circ < \alpha < 20^\circ$ , the drag coefficient increases linearly.

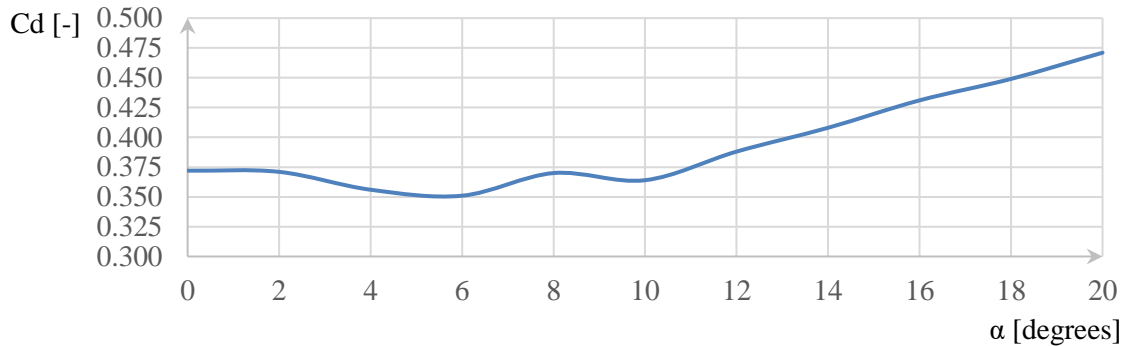


**Figure 10** Variation Cd with angle of deflection,  $0^\circ < \alpha < 20^\circ$

The development of running resistance varies significantly depending on the value of the angle of deviation. The main sources of rolling resistance for a vehicle are: the front and rear wheels, the front pillar associated with the rear-view mirrors and the rear of the vehicle, the latter also being the main source of aerodynamic energy consumption.

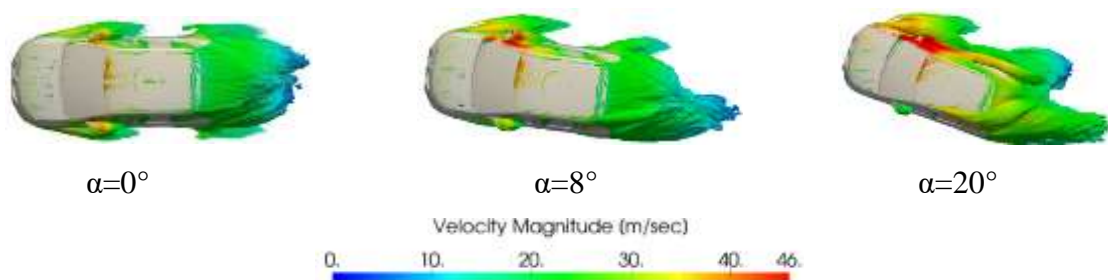


**Figure 11** Evolution of the wale shape of the vehicle with the angle of deflection,  $\alpha$ .

The CdA values for the positive or negative  $\alpha$  angle have slight differences, these are given by the asymmetry of the mechanical parts found under the vehicle body.

Since current research is based on CFD instruments, it is mandatory to associate the results obtained with insight into possible sources of error. An important source is simulation time (i.e. how long air passes by the vehicle), which in the virtual world is fragmented into many small steps called iterations. Exposure to airflow must be long enough to allow resistance forms to form and stabilize. On the other hand, if the exposure to airflow is too long, the recorded data will be too high and the advantage of the CFD instrument will be reduced. For

the current study, simulations were performed at both 250,000 iterations and 500,000 iterations, and figure 12 shows the differences obtained.

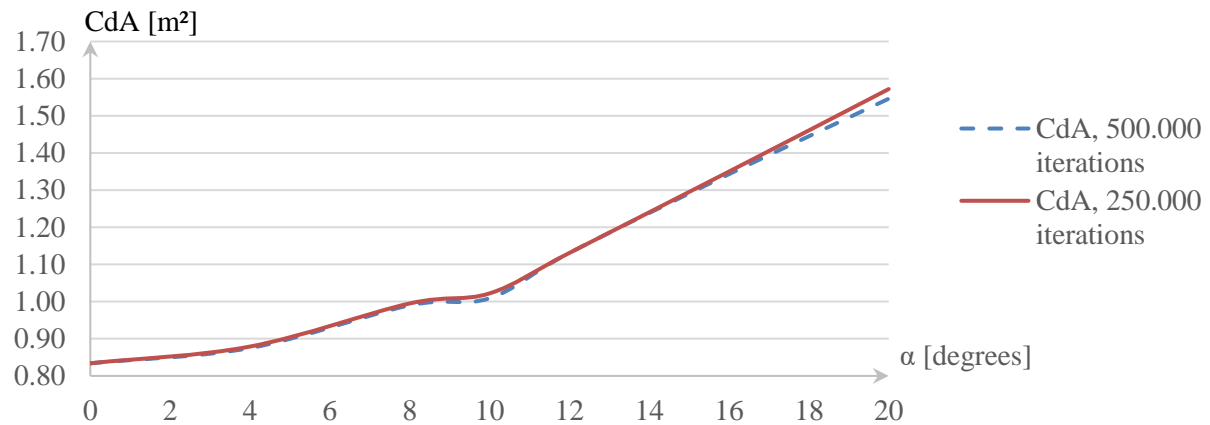


**Figure 12** Cd variation as a function of CFD simulation time

It is considered that the CFD results obtained for a simulation time of 250,000 iterations are valid, considering the purpose of this paper.

The results obtained through CFD simulations show that, for small deflection angles, vehicle performance can be considered uniform up to  $\alpha < 8^\circ$  and after  $\alpha > 10^\circ$  performance degrades in a linear manner.

Next will be considered a standard wheel configuration – 15-inch steel rim without wheel cover and aerodynamic wheel configuration – 15-inch alloy wheel equipped with complete front and rear wheel covers and fairing for the rear wheels, as shown in figure 13.

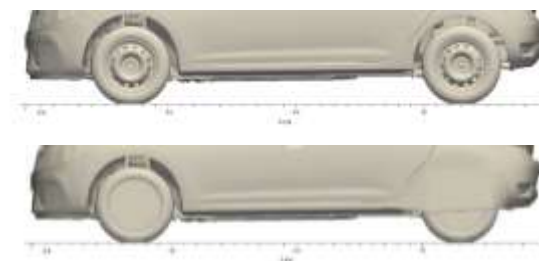


**Figure 13** Studied wheel configurations in crosswind conditions

CFD results are integrated into a graph showing the change in drag coefficient with the angle of deflection. The evolution of Cd can be divided into two main parts, for  $\alpha < 10^\circ$  and for  $\alpha > 10^\circ$ . Cd decreases by 0.020 to  $\alpha = 4^\circ$  and continues slightly to  $\alpha = 8^\circ$ . For  $\alpha = 10^\circ$  a small degradation can be observed, followed by a constant increase in the Cd value. If for  $\alpha < 10^\circ$  it

can be considered that  $C_d$  has on average approximately the same value, for  $\alpha > 10^\circ$  it is obvious that aerodynamic performance degrades without any hint of inclination to lower values.

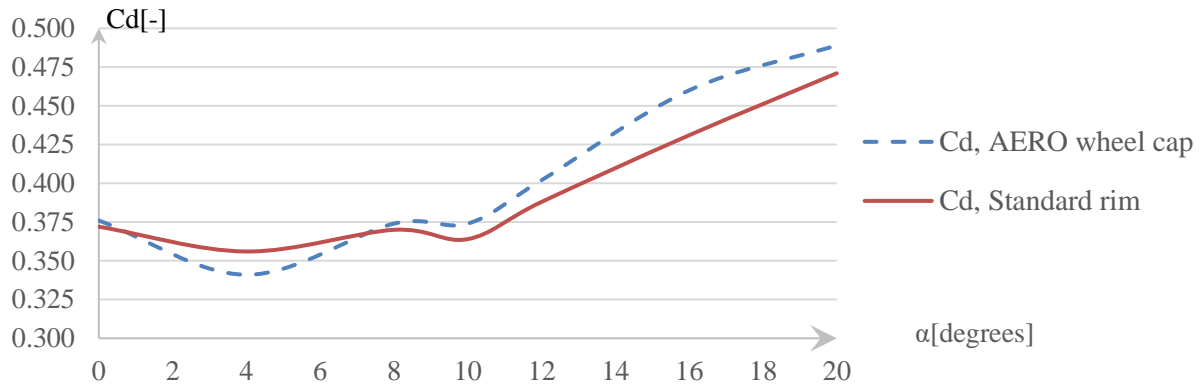


**Figure 14** Variation  $C_d$  with  $\alpha$  for standard and aerodynamic wheels

In order to understand and evaluate the evolution of the drag coefficient, it is necessary to analyse the resistance zones that are developed under different angles of deflection.

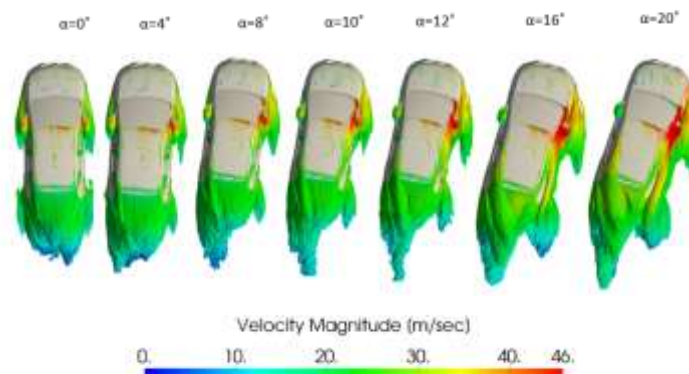


**Figure 15** Wake shape variation with deflection angle,  $\alpha$

For  $\alpha < 10^\circ$  it can be seen that the rear wake is transformed from an almost uniform shape to an asymmetrical shape with a longer but thinner volume. At the same time, the resistance associated with the straight front pillar and exterior mirror intensifies. The oscillation of  $C_d$  as a function of  $\alpha$  can be explained, in this specific case, by the different amount of energy consumed by each mentioned local resistance zone.

For the  $\alpha < 8^\circ$  there is a beneficial effect due to the low energy in the rear resistance, which for vehicles is the most important, although the other areas are still stable and at almost the same energy level. For  $-8^\circ < \alpha < 8^\circ$ , an intensification of the strength of the pillar and front wheel begins to occur. This is how the slight increase in overall  $C_d$  can be explained.

For  $\alpha \geq 10^\circ$ , the main difference lies in the detachment of the local resistance form of the straight pillar. Previous research has indicated an important gain of Cd that can be achieved with the help of the aerodynamic technical definition for wheels: full wheel cover on all four wheels and wheel deflectors for the rear wheels.

As already mentioned, in order to have a better understanding of the total aerodynamic drag of the car, it is necessary to refer to the parameter CdA and not only to Cd. In figure 16, the evolution of CdA by  $\alpha$  can be analyzed.

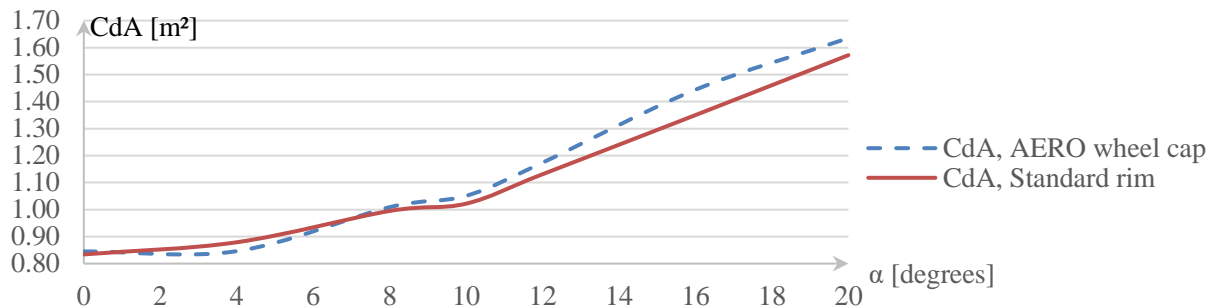


**Figure 16** CdA variation with  $\alpha$  for standard and aerodynamic wheel design

Optimised solutions for the current homologation process may pose significant challenges for new procedures such as RDE (Real Driving Emissions). However, it is considered mandatory to include active aerodynamic elements in the technical definition of the vehicle in order to comply with the tough CAFÉ (Corporate average fuel economy) rules.

On the basis of the aerodynamic studies submitted, which assess the basic performance of three body types widely available for general use but also for intervention vehicles, plus favourable results for some of the wheel scenarios studied (both in the standard longitudinal wind direction and in crosswind), it is decided to further assess the possible aerodynamic benefit of replacing fairings under the bodywork with extended surface parts and a improved flatness of wheels

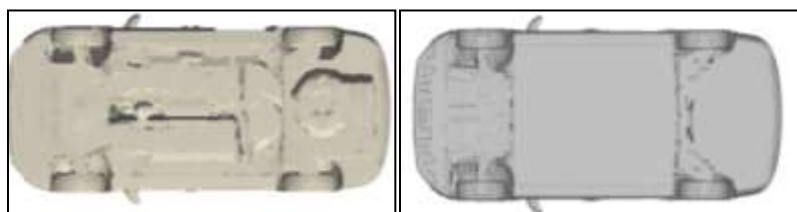


**Figure 17** Standard fairings under the bodywork versus proposed fairings

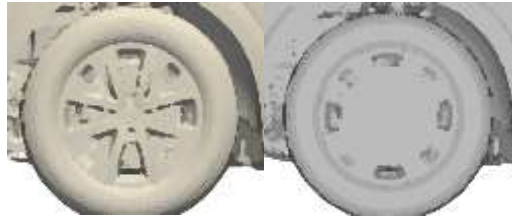


**Figure 18** Standard wheel (left) versus proposed aerodynamic rim (right)

CFD simulations performed on each body type, with technical developments detailed above, indicate a different influence of added parts on the overall performance of CdA, as shown in Table 3.

**Table 3** CdA results for optimised technical definition, in relation to base and intervention vehicle

Case studied	Sedan "base vehicle"	Sedan "emergency vehicle"	Sedan "optimised vehicle"
SCx [m <sup>2</sup> ]	0.659	0.753	0.708
$\Delta$ SCx [m <sup>2</sup> ]	-	+ 0.094	+ 0.049
$\Delta$ SCx [%]	-	+ 14	+7.44
Case studied	Hatch back "base vehicle"	Hatch back "emergency vehicle"	Hatch back "optimised vehicle"
SCx [m <sup>2</sup> ]	0.836	0.910	0.899
$\Delta$ SCx [m <sup>2</sup> ]	-	+0.074	+ 0.063
$\Delta$ SCx [%]	-	+8.8	+7.54
Case studied	SUV "base vehicle"	SUV "emergency vehicle"	SUV "optimised vehicle"
SCx [m <sup>2</sup> ]	1.000	1.059	0.998
$\Delta$ SCx [m <sup>2</sup> ]	-	+0.059	-0.002
$\Delta$ SCx [%]	-	+5.8	- 0.02

Analyzing the results obtained, several conclusions can be drawn. First, as expected, a newly introduced element will not have the same effect on different body types. This is due to a different shape of the vehicle and the speed of airflow above and below the body (providing a specific shape and dimensions of rear wake). Consequently, for better results, body-specific customisation is required. Secondly, the aerodynamic drag of the light warning device can be

fully compensated (SUV body – balanced rear wake) or halved (sedan body – slightly unbalanced rear wake in the downward direction) by using a relatively simple body kit for intervention vehicles.

When it comes to the hatch back body type, further studies will need to be carried out to identify a suitable set of parts to match the base vehicle's wake, as the current configuration has an unbalanced, large-sized rear wake. Some options that will be tested to see if they improve the wake for hatch rear intervention vehicles are: partial body covering, addition of deflectors on fairings or extension of the rear upper diffuser.

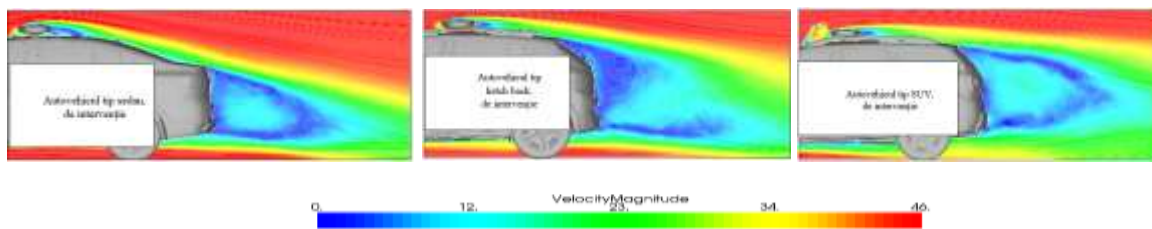


**Figure 20** Rear wake of optimised intervention vehicles

The present study focused on a generic light warning device and not on aerodynamically optimised ones, as the first mentioned ones are more widely available, are already applied to most intervention vehicles, are easy to install and have a low risk of not complying with the laws applied in this field.

In addition, for the CFD study carried out on passenger vehicles such as sedans, hatch backs, SUVs and how light warning devices influence aerodynamic performance, further studies have already been initiated for the field of heavy commercial vehicles such as trucks. Even if still at an early stage, a summary of the first steps taken with fellow researchers in the field of automotive aerodynamics is presented. [75] [76]

The trucks have relatively large dimensions considering the automotive segment of transport, a fact imposed by their generic destination for freight transport, a category chosen to be of primary interest due to their relatively high speeds and large number of working hours. Therefore, from an aerodynamic point of view, these vehicles have the disadvantage of generating high rolling resistance.

Eleven study cases are defined for the roof warning light, devices to be mounted on a generic tractor cab.



CFD simulations are carried out in the virtual environment and only the tractor unit will be used, without applying a semi-trailer due to the fact that the area of interest is on the roof of the cab.

For the interpretation of the results, the use of current, velocity vectors and pressures. Also, for a good visibility of the analyzed parameters, such as current lines and speed vectors, it was chosen to exemplify them on a ZOY plane at the YO coordinate where in almost all cases there are elements that disturb the air flow.

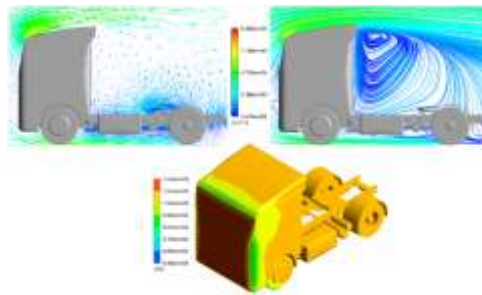


**Figure 21** Air flow for the truck cab

Based on the numerical values and interpretation of air flows for the studied cases, it can be said that light warning modules degrade the aerodynamic performance of trucks. Consequently, integrating them into the roof deflector can be considered a viable option. Configurations 7 to 11 allow by the nature of the construction better airflow, therefore higher aerodynamic performance than in previous cases.

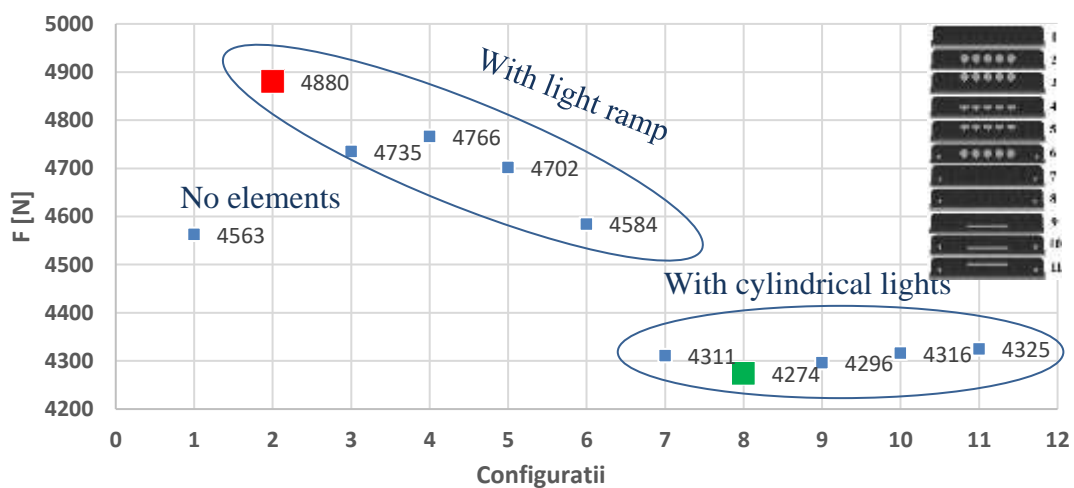


**Figure 22** X-axis force values for the studied configurations

## 6. EXPERIMENTAL RESULTS

The experimental results and related conclusions, obtained in the virtual environment and detailed in Chapter 5, are validated by performing physical experiments as close as possible to the conditions of the real environment, but under laboratory conditions.

The parameters controlled in making physical measurements are those of the ambient air in the test chamber such as: air temperature of 20 degrees Celsius, air density of 1.2041 kg / m<sup>3</sup>, and the preset air travel speed is 140 km / h.

The paper presents three cases measured in order to correlate virtual measurements. The scenarios chosen are identified as those with the centrally mounted light warning device because the study detailed in Chapter 5 identified these cases as being among the most beneficial for the aerodynamic drag of emergency vehicles on the one hand and on the other hand because it is the most common scenario for intervention vehicles.

To carry out the test, the sedan was introduced into the enclosure and was connected to the measuring module to carry out the first reference test. Then, maintaining exactly the same position of the vehicle, the warning light described in Chapter 5 was fitted in the middle position. The measurement was thus carried out with the device mounted and the new result for the drag coefficient was recorded. The difference between the two values is analyzed and then compared with the result obtained under the same conditions, in a virtual environment.

The test procedure is repeated under the same conditions for all three bodies, sedan, hatch back and SUV, analyzed in the paper. The location of the light warning device in the center area is illustrated in figure 23 for the three types of body analysed.



**Figure 23** Location of light warning device

Physical measurements indicate that the light warning device used, in the mid-mounting position, for a sedan brings about a degradation of 18 %. If we refer to measurements made under virtual conditions, through CFD simulations, the degradation obtained under the same conditions is 14%. In this case, there is a difference of 4 percentage points between the 2 measurements made.

In the case of a hatch back vehicle, by applying the same test conditions, the degradation caused by the warning light device was of 8 %. In this case, we can notice a difference of only 0.8 percentage points compared to the results obtained in the virtual environment.

The case of the SUV indicates by physical measurement of the drag coefficient a degradation of 5.5%, while the numerical results presented in Chapter 5 indicated a degradation of 5.8% in the virtual environment. The difference between the two measurements is only 0.3 percentage points.

The values obtained for the scenarios presented confirm the conclusions listed in Chapter 5, namely:

- Additional devices located on the roof of cars have a negative influence on aerodynamic drag because they affect the balance of airflow for the base car (without added devices)
- The light warning device has a greater influence on sedans compared to other body types.
- The influence of the additional device decreases in weight from the sedan to the rear hatch and finally to the SUV-type body, due to the different rear wake and the interaction between it and the local wake of the light warning device.

Considering the results of the physical measurements, it is considered that the study conducted in the virtual environment is relevant and its conclusions are valid.

## **7. CONCLUSIONS, PERSONAL CONTRIBUTIONS and FUTURE RESEARCH DIRECTIONS**

The paper addressed the influence of roof-mounted warning devices specific to intervention vehicles on air flow and thus on the aerodynamic performance. This subject was chosen for the study because an increased aerodynamic drag leads to higher emissions and therefore to an amplified negative effect on the environment and human health. Current legislation excludes the emergency vehicles from the rules and penalties associated with an increased amount of emissions. However, in the context of the decarbonization of the entire transport segment, a new, more restrictive legislative framework is also expected to be implemented for intervention vehicles.

With the help of phenomena associated with air flow around vehicles and methods for measuring aerodynamic drag, a study was conducted using the CFD method to analyze the aerodynamics of sedans, hatch backs and SUVs. These typologies were chosen because they are often used in urban or suburban environments, by institutions or other authorities requiring the use of vehicles with warning equipment.

The study consisted of first assessing the basic aerodynamic performance of vehicles without roof-mounted warning devices. It was found that the sedan has the best aerodynamic performance of the 3 body types listed. This is mainly due to a reduced rear surface, approaching the shape of a drop of falling water. Unlike the sedan, the hatch back has an increased rear surface area and therefore an increased rear wake in size. Thus, its aerodynamic drag is considerably higher than in the case of the sedan. Regarding the SUV, there was an increase in aerodynamic drag compared to the sedan, but also compared to the hatch back. Even if not a huge difference from the hatch back was recorded, the measured values for the SUV-

specific drag coefficient indicate both a larger rear wake and the negative effect on the balance of the rear wake associated with higher ground clearance.

The intermediate stage of the work presented the results of an extensive study on the aerodynamics of the wheels and wheel arch. The aim was to determine to what extent optimizations made in this area can improve the aerodynamic drag of vehicles. This topic was chosen on the assumption that potential modifications are easy to make without requiring significant changes to the bodywork or basic structure of the vehicle.

The extensive studies carried out on the aerodynamics of vehicle wheels have been transposed both for the scenario in which the air flow comes from the front, but also for the scenario of distinct location between the vehicle and the air flow, i.e. crosswind conditions. This extension of the work was considered necessary for a more complete evaluation of the aerodynamics of the vehicle and the analysis of the identified benefits for the air flow both on the X-axis and the variation by  $\pm 20^\circ$  compared to the X-axis. In addition, studying the vehicles' aerodynamics in a scenario with crosswind conditions is necessary also due to the check of emissions in real-life conditions carried out by the authorities using the RDE methods.

In crosswind determinations, an interesting effect was found when comparing the definition of standard wheel with that one defined as aerodynamic. If for relatively small angles the aerodynamic wheel had a positive effect, it was found that when increasing the lateral angle, the increased design area effect led to an overall negative effect and thus to an increase in aerodynamic drag. The main conclusion is that, for a complete and accurate overview of aerodynamic performance, it is not enough to validate only with the airflow strictly aligned with the X-axis of the vehicle, but it is necessary to evaluate and determine the values of the drag coefficient also in crosswind conditions. This component can significantly contribute to reducing the difference between the fuel consumption announced by the manufacturer (determined under laboratory conditions) and the fuel consumption registered by the customer when operating the vehicle under normal conditions. Of course, aerodynamic drag is only one of the components needed to be studied to reduce the difference in fuel consumption.

The CFD study consisted of evaluating the performance of intervention vehicles for the three types of body mentioned and an analysis of the main scenarios for mounting the light warning device: anterior, median and rear. The aerodynamic effects encountered locally in the area of the roof-mounted device, as well as the effect on the rear wake of each vehicle, are analyses based on the air flow, vorticity and associated pressure deficit. For all cases, however, mounting the light warning device in the front position was the worst due to its positioning in

the path of high-speed airflow coming from the windscreen area, thus leading to a local wake amplified in size and energy.

The final stage of the study consisted in trying to improve the aerodynamic resistance of intervention vehicles with elements considered easy to apply such as: optimizing the wheel trim and fixed elements located under the vehicle (fairings), by extending them and ensuring increased flatness. The shape of vehicle fairings is generally conditioned by factors such as the material from which they are made (i.e. whether or not the systems under the vehicle can be approached to hot sources) and constraints linked to their architecture or mounting possibility.

The CFD results obtained through the set of simulations carried out on intervention vehicles with mid-positioned light warning device, low porosity wheel trim and aerodynamically optimized fairings indicated the possibility of reducing aerodynamic drag.

Thus, for the sedan, the effect of additional aerodynamic elements made it possible to partially compensate for the presence of the warning light. The numerical results indicated a reduction of almost 50% in the effect initially created by the presence of the light warning device, which underlines on the one hand the contribution of the study carried out, but also the possible prospects of further reduction of aerodynamic drag. In the case of the hatch back, the same trend was encountered, but with a significantly reduced effect, this being due to a poor rear wake. The shape of the rear wake and its balance, in the case of the hatch back, are deficient compared to the sedan and therefore the effect of the light warning device is different in the 2 cases. For the hatch back, additional aerodynamic optimization elements are required to enable the same gain as in the sedan. The negative eddy effect associated with a large rear surface is even more emphasized in the case of an SUV, where the application of those optimization elements has no effect. This result is because the optimized elements have relatively little influence on the overall SUV aerodynamics equation. For this case, it is therefore necessary to identify other optimization areas to be able to reduce aerodynamic drag.

The study concludes that light warning devices have a significant influence on vehicles, and the study of sedan, hatch back and SUV bodies is vital for reducing fuel consumption and thus associated emissions. This can lead to a beneficial financial effect, but also an important contribution to the decarbonization of transport, mainly in urban and suburban areas.

The correlation of the numerical results obtained for the aerodynamic performance of the intervention vehicles was achieved through physical measurement experiments on 1:1 scale =âvehicles of sedan, hatch back and SUV type. The measurement conditions were similar between virtual and physical methods to allow validation of the study performed. Following the measurements, it was found that for the sedan the difference between the 2 measurements

is 4 percentage points, for the hatch back car 0.8 percentage points, and for the SUV the difference is only 0.3 percentage points. These results are mainly due to the balance sensitivity for the rear wake of each vehicle type. Since the sedan has better performance but a more sensitive balance, the numerical method does not completely capture its phenomenology as is achieved in the physical experiment. But for the hatch back and SUV, where the wake is larger but more stable, the numerical and physical methods showed very close results.

The continuous transformation of the automotive industry, the desire to make transport more efficient, but also the obligation to reduce emissions lead to the need for aerodynamic studies, such as this work, on intervention vehicles equipped with light warning devices. The current study stands out for addressing this topic for sedan, hatch back and SUV body types, as no similar works published in the literature have been identified. The degree of uniqueness of the presented subject and the large use of these types of bodies for intervention vehicles indicate an important contribution to the field.

The paper not only presents a global analysis of the aerodynamics of sedans, hatch backs and SUVs, but also extensively studies the local aerodynamics of vehicle wheels and their influence on overall performance. The contributions made consist in creating a detailed overview of air flow in the wheel rim area, by studying the porosity and flatness factors of distinct scenarios, which can be correlated with the models currently used in the automotive industry.

This paper presents for the first time in our country the results of the research carried out, regarding measurements for the light warning device for sedan, hatch back and SUV, not only in the virtual environment by CFD method, but also correlated with physical measurements on vehicles scale 1:1. The present paper can be a reference study in the case of the study of fuel reduction for vehicles used by police, constabulary, patient transport or firefighters, naming only a few institutions that frequently use vehicles of the type studied and presented in the current paper.

The studies will be continued primarily with the analysis of accessories that can improve the aerodynamic resistance of sedans with light warning device, but especially of accessories necessary for hatch back and SUV vehicles with light warning device. The aim remains to identify a set of elements to cancel out the negative effect of the light warning device on aerodynamic performance.

Another research path is the implementation of active aerodynamic elements, such as trim wheels whose porosity that can be varied, so that performance is optimized not only for

the theoretical airflow situation aligned with the vehicle's X-axis, but also for various real-life situations where crosswind occurs.

The research may also extend to other body types used by authorities and institutions, such as station wagons, vans or pick-ups. In this respect, collaborations already started aim at studying the aerodynamic of heavy tractor vehicles and the influence of the various light warning devices that can be used, as presented at the end of the paper.

The topic of aerodynamics of intervention vehicles is considered relevant and of real interest for the efficiency of the transport segment, optimizing the costs associated with the fuel consumed, but also for reducing emissions and influence on the environment. In this context, the study presents the first steps taken, future research paths, aiming to extend physical validations for a complete correlation, so that the material can be considered a reference point in this field.

## References

1. Reducerea emisiilor de carbon: obiective și politici ale UE, Parlamentul European, aprilie 2023
2. Michelle Mongo, Fateh Belaïd, Boumediene Ramdani, The effects of environmental innovations on CO2 emissions: Empirical evidence from Europe (Efectele inovațiilor de mediu asupra emisiilor de CO2: dovezi empirice din Europa), Environmental Science & Policy, volumul 118, 2021, paginile 1-9, ISSN 1462-9011,
3. [https://single-market-economy.ec.europa.eu/sectors/automotive-industry/vehicle-categories\\_en](https://single-market-economy.ec.europa.eu/sectors/automotive-industry/vehicle-categories_en)
4. [https://climate.ec.europa.eu/system/files/2023-02/policy\\_transport\\_hdv\\_20230214\\_proposal\\_en\\_0.pdf](https://climate.ec.europa.eu/system/files/2023-02/policy_transport_hdv_20230214_proposal_en_0.pdf)
5. John D. Anderson Jr., O istorie a aerodinamicii și impactul acesteia asupra mașinilor zburătoare, Universitatea din Maryland, 2001, ISBN 0521669553
6. <https://www.britannica.com/topic/Lilienthal-standard-glider>
7. [https://www.wright-brothers.org/History\\_Wing/History\\_of\\_the\\_Airplane/Doers\\_and\\_Dreamers/Wright\\_Smithsonian\\_Controversy/00\\_Wright\\_Smithsonian\\_Controversy\\_Intro.htm](https://www.wright-brothers.org/History_Wing/History_of_the_Airplane/Doers_and_Dreamers/Wright_Smithsonian_Controversy/00_Wright_Smithsonian_Controversy_Intro.htm)
8. Oliviu SUGAR GABOR, Modelul liniei de ridicare neliniare folosind o formulare vectorială a teoremei instabile Kutta-Joukowski, Inginerie aeronautică și mecanică, Școala de calcul, știință și inginerie, Universitatea din Salford, DOI: 10.13111/20668201.2019.11.1.15, Conferința Internațională de Științe Aeronautice "AEROSPATIAL 2018"
9. Furoni, D & Lima, Ernani & Anderson, Fabiana & Ribeiro, D & Almeida, Franciana & Pedrochi, Francielle & Sato, Gisele & Philippsen, Gustavo & Max, Dearo & Simonetti, Iara & Mantovani, Antonio & Maeda, Kelly & Christine, D & Silva, Michel & Zan, Marcelo & Freitas, D & Andrade, Bordim & Sanches, Cristina & Oliveira, De & Neves, Semn. (2005). SANTOS-DUMONT S & D - danhoni. 10.13140/RG.2.2.18475.46885.
10. <https://historyforce.com/20-romanian-inventors-and-their-great-inventions/>
11. <https://www.britannica.com/technology/automotive-industry/The-modern-industry>
12. Curs „DINAMICA AUTOVEHICULELOR”, Prof. Dr. Ing. Cristian Andreescu, Facultatea Transporturi, Dept. Autovehicule Rutiere, UPB, 2012-2013
13. E I Houghton, P W Carpenter "Aerodinamica pentru studenții ingineri", ediția a 5-a, Universitatea din Warwick
14. J. Pavlovic, B. Ciuffo, G. Fontaras, V. Valverde, A. Marotta, How much difference in type-approval CO2 emissions from passenger cars in Europe may be expected from change to the new test procedure (NEDC vs. WLTP)?, Transportation Research Part A: Policy and Practice, Volume 111, 2018, Pages 136-147, ISSN 0965-8564
15. Saša VASILJEVIĆ, Nataša ALEKSIĆ, Dragan RAJKOVIĆ, Rade ĐUKIĆ, Milovan ŠARENAC, Nevena BANKOVIĆ, BENEFICIILE APLICĂRII TEHNOLOGIEI CAD/CAE ÎN DEZVOLTAREA VEHICULELOR DIN INDUSTRIA AUTO, A CTA TECHNICA CORVINIENSIS – Buletin de inginerie, volumul XI, 2018, Capitolul 2
16. Keck, Helmut și bolnav, Mirjam, Treizeci de ani de simulare a debitului numeric în turbomașini hidraulice, Acta Mechanica. 2008, 201. 211-229. 10.1007/S00707-008-0060-4



17. Denton J. D., 2010, "Unele limitări ale CFD-urilor turbomachinery". ASME. Turbo Expo: Putere pentru uscat, mare și aer, Vol. 7, doi: 10.1115 / GT2010-22540.
18. R L IOVĂNEL, Simularea numerică a debitului într-o turbină KAPLAN, teză de doctorat, București, 2018
19. Wang, B., Wang, B., Lv, B., Wang, R. (2022). Impactul gazelor de eșapament ale autovehiculelor asupra calității aerului dintr-un oraș urban. *Aerosol Air Qual. Rez.* 22, 220213. <https://doi.org/10.4209/aaqr.220213>
20. Wolf-Heinrich Hucho, Aerodinamica vehiculelor rutiere: de la mecanica fluidelor la ingineria vehiculelor, ediția a 4-a,
21. Babinsky, Holger. (2003). Cum funcționează aripile?, 38. 497. 10.1088/0031-9120/38/6/001.
22. <https://www.greenoptimistic.com/100-year-old-aerodynamics-problem-solved-could-increase-mpg-dramatically-20080927/>
23. Jones Classical Aerodynamic Theory, Standford Course
24. <https://www1.grc.nasa.gov/beginners-guide-to-aeronautics/boundary-layer/>
25. Pijush K. Kundu, Ira M. Cohen, David R. Dowling, Capitolul 9 - Straturi limită și subiecte conexe, Editor(i): Fluid Mechanics (ediția a cincea), Academic Press, 2012, , ISBN 9780123821003,
26. V.N. Constantinescu, St. Galetuse, Mecanica fluidelor și elemente de aerodinamica, Didactica și Pedagogica, 1983
27. Uruba, Vaclav. (2018). Despre interpretarea fizică a numărului Reynolds. *Lucrările conferinței AIP.* 2000. 020019. 10.1063/1.5049926.
28. Aerodinamica mașinilor de curse, Joseph Katz, ediția 1
29. Mishra, Pankaj și Aharwal, K. (2018). O revizuire a selecției modelului de turbulență pentru analiza CFD a fluxului de aer într-un depozit frigorific. *Seria de conferințe IOP: Știința și ingineria materialelor.* 402. 012145. 10.1088/1757-899X/402/1/012145.
30. Charles N. Eastlake, Viziunea unui aerodinamician asupra lui Lift, Bernoulli și Newton
31. <https://racecar-engineering.telegraph.co.uk/articles/f1-ferrari-sf90-testing-update/>
32. <https://www.aip-automotive.de/en/Products/Test-Stands/RESEARCH-DEVELOPMENT/Wind-Tunnel-Balance>
33. Barlow, Jewel B., Rae, William H., Pope, Alan. Testarea tunelului aerodinamic la viteză redusă. *Regatul Unit: Wiley*, 1999.
34. <https://www.curbsideclassic.com/automotive-histories/automotive-history-an-illustrated-history-of-automotive-aerodynamics-part-1-1899-1939/>
35. <https://www.topgear.com/car-news/electric/these-are-10-most-aerodynamically-efficient-evs-sale-today>
36. <https://ceautoclassic.eu/persu-forgotten-streamliner-pioneer/>
37. Obidi, T. Yomi. Teoria și aplicațiile aerodinamicii pentru vehiculele terestre. *Statele Unite: SAE International*, 2014.
38. <https://www.serus-dacia.ro/noul-sandero-stepway>
39. <https://heycar.co.uk/blog/new-2023-toyota-prius>
40. <https://configurator.porsche.com/en-US/model/992120/option/1NV>
41. <https://newsroom.toyota.eu/prius-plug-in-hybrid/>

42. <https://cnevpost.com/2023/01/11/regulatory-filing-heres-what-nios-new-es6-looks-like/>
43. <https://whyisthisinteresting.substack.com/p/the-aero-wheel-edition>
44. <https://ehfcv.com/air-curtains/>
45. <https://insideevs.com/news/520224/doug-demuro-reviews-vw-xl1/>
46. <https://www.magna.com/products/body-exterior-structures/active-aerodynamics>
47. <https://www.car-engineer.com/renault-eolab-aerodynamics-features/>
48. <https://www.digitaltrends.com/cars/road-rave-how-aerodynamics-is-reshaping-the-car-industry/>
49. <https://g05.bimmerpost.com/forums/showthread.php?t=1612428>
50. Taherkhani, Sam și de Boer, Greg și Gaskell, P.H. și Gilkeson, C.A. și Hewson, Rob și A, Keech și Thompson, Harvey și Toropov, Vassili. (2015). Reducerea rezistenței aerodinamice a vehiculelor de intervenție în caz de urgență. Progrese în ingineria automobilelor. 4. 1000122. 10.4172/2167-7670.1000122.
51. Tendințe de îmbunătățire pentru motoarele cu ardere internă. Croația: IntechOpen, 2018.
52. Anil K. Madhusudhanan, Daniel Ainalis, Xiaoxiang Na, Isabel Vallina Garcia, Michael Sutcliffe, David Cebon, Efectele modificărilor semiremorcii asupra consumului de combustibil HGV, Cercetare în domeniul transporturilor Partea D: Transport și mediu, volumul 92, 2021, 102717, ISSN 1361-9209,
53. Taherkhani, Sam. (2015). Optimizarea bazată pe dinamica fluidelor computaționale a vehiculelor de intervenție în caz de urgență.
54. Bayraktar, I. și T. Bayraktar, Ghid pentru simularea CFD a aerodinamicii vehiculelor terestre. SAE International 10.4271/2006-01-3544, 2006.
55. Aider, J. și J.F. Beaudoin, reducerea rezistenței la înaintare și ridicare a unui corp de cacealma 3D folosind clapete. Experimente în fluid 10.1007/s00348-007-0392-1, 2008.
56. David C. Brock, Înțelegerea legii lui Moore: patru decenii de inovație. Statele Unite: Fundația Patrimoniului Chimic, 2006.
57. Tudor BARACU, Ecuatiile Navier-Stokes, Universitatea Politehnica din București
58. Jurij SODJA, Modele de turbulență în CFD, Universitatea din Ljubljana, Facultatea de matematică și fizică Departamentul de fizică, Introducere
59. Jurij SODJA, Modele de turbulență în CFD, Universitatea din Ljubljana, Facultatea de matematică și fizică, Departamentul de Fizică, Ljubljana, martie 2007
60. Dieter A. Wolf-Gladrow Alfred Wegener Institutul pentru Polare și Marină
61. Dieter A. Wolf-Gladrow , cercetare, Automate celulare cu zăbrele și modele Boltzmann cu zăbrele - o introducere, Germania,
62. Luan, Huan-Bo și Xu, Hui și Chen, Li și Sun, Dongliang și Tao, Wen-Quan. (2010). Ilustrații numerice ale cuplării dintre metoda Boltzmann cu zăbrele și metodele macronumerice de tip finit. Transfer numeric de căldură. Partea B: Fundamente. 147-171. 10.1080/15421400903579929.
63. [https://www.soufflerie2a.com/en/moyens\\_soufflerie/soufflerie-echelle-11-561.html](https://www.soufflerie2a.com/en/moyens_soufflerie/soufflerie-echelle-11-561.html)
- 64. L Ilea, D Iozsa și G Fratila , Modelarea unui tunel aerodinamic virtual pentru masuratori aerodinamice ale vehiculelor, IOP Conf. Ser.: Mater. Sci. Ing. 1220 012027, 10.1088/1757-899X/1220/1/012027**
65. <https://www.soufflerie2a.com/en/>

66. [https://www.soufflerie2a.com/en/moyens\\_soufflerie/soufflerie-echelle-11-561.html](https://www.soufflerie2a.com/en/moyens_soufflerie/soufflerie-echelle-11-561.html)
67. Manual de utilizare ANSA
68. Emmanuel Lévêque, F. Toschi, Liang Shao, Jean-Pierre Bertoglio. Modelul Smagorinsky îmbunătățit prin forfecare pentru simularea turbionară a fluxurilor turbulente legate de pereți. Jurnalul de mecanică a fluidelor, 2007, 570, pp.491-502. ff10.1017/S0022112006003429ff. fhal-00272169f
69. Ilea, L., Iozsa, D., Stan, C., Fratila, G. (2019). impactul jantei roții asupra aerodinamicii vehiculelor de pasageri. În: Burnete, N., Varga, B. (eds) Proceedings of the 4th International Congress of Automotive and Transport Engineering (AMMA 2018). AMMA2018 2018. Proceduri în ingineria auto. Springer, Cham. [https://doi.org/10.1007/978-3-319-94409-8\\_11](https://doi.org/10.1007/978-3-319-94409-8_11)
70. D Iozsa, L Ilea și G Fratila, Influența luminilor de avertizare pentru vehiculele de intervenție asupra performanțelor aerodinamice, IOP Conf. Ser.: Mater. Sci. Ing. 997 012118, 10.1088/1757-899X/997/1/012118
71. <https://www.mvslight.com/Product/15-inch-E--Type-Multi-LED-Light-Bar/29/>
72. L Ilea, D Iozsa și G Fratila, Un studiu teoretic aerodinamic privind accesoriile exterioare ale vehiculelor de intervenție, 2022 IOP Conf. Ser.: Mater. Sci. Ing. 1235 012034, DOI 10.1088/1757-899X/1235/1/012034
73. L Ilea și D Iozsa, Aerodinamica roților și impactul asupra coeficientului aerodinamic al vehiculelor de pasageri, 2018 IOP Conf. Ser.: Mater. Sci. Ing. 444 072005, DOI 10.1088/1757-899X/444/7/072005
74. Ilea, L., Iozsa, D., Stan, C., Teodorescu, C. (2020). Studiu CFD privind performanța aerodinamică a roților în condiții de vânt lateral pentru un vehicul hatchback. În: Dumitru, I., Covaciu, D., Răcilă, L., Roșca, A. (eds) The 30th SIAR International Congress of Automotive and Transport Engineering. SMAT 2019. Springer, Cham. [https://doi.org/10.1007/978-3-030-32564-0\\_15](https://doi.org/10.1007/978-3-030-32564-0_15)
75. Influența fluxului de aer din zonele laterale ale unui cap tractor asupra performanțelor aerodinamice ale acestuia, E M Vieru, D Iozsa, L Ilea și G Frățilă / ACME 2022 / E M Vieru et al 2022 IOP Conf. Ser.: Mater. Sci. Eng. 1262 012075
76. The influence of warning lights on the truck cabins on aerodynamic performance, E M Vieru, D Iozsa, L Ilea and G Frățilă / EAEC - MVT 2022 (in curs de publicare)
77. Adithya Hariram, Thorsten Koch, Björn Mårdberg , Jan Kyncl, Un studiu privind opțiunile de îmbunătățire a profilului aerodinamic al vehiculelor grele în Europa, 2019
78. Anexa 64: Regulamentul nr. 65, Dispoziții uniforme privind omologarea lămpilor speciale de avertizare pentru autovehicule și remorcile acestora, Organizația Națiunilor Unite, 7 decembrie 2011
79. <https://www.dauto.ro/bara-proiectoare-volvo-fh4-euro-6-globetrotter-xl-3.html?>
80. <https://www.paul-trans.ro/img/56921agabaritic.jpg>
81. <https://www.obiectivdesuceava.ro/local/la-noapte-si-maine-traffic-ingreunat-din-cauza-a-doua-transporturi-agabaritice-care-vor-strabate-judetul-suceava/>
82. Liu, Y. și Glass, G. (2013). Efectele densității ochiului de plasă asupra analizei elementelor finite. Seria de hârtie tehnică SAE. doi:10.4271/2013-01-1375 Liu, Y. și

- Glass, G. (2013). Efectele densității ochiului de plasă asupra analizei elementelor finite. Seria de hârtie tehnică SAE. doi:10.4271/2013-01-1375
83. Suresh, K. și Regalla, S. P. (2014). Efectul parametrilor ochiului de plasă în simularea cu elemente finite a procesului de formare a foilor incrementale într-un singur punct. Procedia Știința Materialelor, doi: 10.1016/j.mspro.2014.07.048
84. Mihail Daniel Iozsa, Caroserii pentru autovehicule rutiere, Editura Politehnica Press, Bucuresti, 2016
- 85. D Iozsa , Study on the Influence of the Convoy Rolling over Aerodynamic Resistance, D Iozsa et al 2017 IOP Conf. Ser.: Mater. Sci. Eng. 252 012035**
86. <https://www.aip-automotive.de/en/Products/Test-Stands/RESEARCH-DEVELOPMENT/Wind-Tunnel-Balance>
87. <https://jaimeirastorza.wordpress.com/2014/08/22/a-primer-on-automotive-wind-tunnels/>
88. <https://www.directindustry.com/cat/force-measurement-BO.html>
89. [https://www.jstor.org/stable/44724870?read-now=1&seq=9#page\\_scan\\_tab\\_contents](https://www.jstor.org/stable/44724870?read-now=1&seq=9#page_scan_tab_contents)
90. <https://uk.motor1.com/news/672374/for-new-rolling-road-wind-tunnel-200mph/>
91. <https://arstechnica.com/cars/2022/03/honda-just-built-the-worlds-most-advanced-wind-tunnel-in-ohio/>